

Frequency-dependent sites amplifications evaluated from well-logging data in central Taiwan

Ming-Wey Huang,¹ Jeen-Hwa Wang,² Hung-Hao Hsieh,³ Kuo-Liang Wen,^{1,3} and Kuo-Fong Ma¹

Received 17 May 2005; revised 7 September 2005; accepted 28 September 2005; published 3 November 2005.

[1] Based on the quarter-wavelength approximation by Boore and Joyner (1997), the frequent-dependent site amplifications at 87 free-field strong-motion stations in central Taiwan from borehole data are evaluated. Results show that the amplifications increase with frequency, and the amplification is larger at the sites in the Western Plain with Holocene alluvium than at those in the Western Foothill with Pleistocene and Miocene formations.

Citation: Huang, M.-W., J.-H. Wang, H.-H. Hsieh, K.-L. Wen, and K.-F. Ma (2005), Frequency-dependent sites amplifications evaluated from well-logging data in central Taiwan, *Geophys. Res. Lett.*, 32, L21302, doi:10.1029/2005GL023527.

1. Introduction

[2] The site effect remarkably affects the ground motions, thus influencing the estimation of source parameters [cf. Pérez-Campos *et al.*, 2003]. The seismic waves will be amplified when they propagate through the low-shear-velocity and low-density layers. Amplification of seismic waves is usually a function of frequency, and stronger at a soil site than at a rock one. The seismic stations are commonly built on both the rock and soil sites. Thus, the corrections of wave amplitudes must be done before the seismic data are used to estimate source parameters.

[3] Basically, three ways are applied to evaluate the site effects from seismic data. The first way [cf. Zhang, 2004] is the comparison of the Fourier amplitude spectrum at a site to that at a reference hard-rock reference site, with nearly flat response. It is not easy to locate a perfect reference site. The second way [cf. Lermo and Chávez-García, 1993] is the calculation of horizontal-to-vertical spectral ratio at a site. The third way [cf. Atkinson and Cassidy, 2000; Sokolov *et al.*, 2004] is the division of the Fourier amplitude spectrum of ground motions by that simulated from a very-hard-rock model, which is assumed to have no site effects. For this way, the precise source and path effects are needed.

[4] From surficial geology in Taiwan, Lee *et al.* [2001] classified 708 free-field strong-motion station sites into three categories, i.e. classes C, D, and E, using a scheme compatible with the 1997 Uniform Building Code (UBC) provisions. They also studied the response spectra for $f \geq$

0.3 Hz and the horizontal-to-vertical spectral ratios for $0.3 \leq f \leq 33.3$ Hz. Sokolov *et al.* [2004] established the empirical amplification functions in the frequency range 0.1–10 Hz as the ratio between Fourier amplitude spectra of recorded accelerograms and spectra simulated based on a hypothetical very hard rock model. Zhang [2004] evaluated the site amplification, with attenuation, for $0.7 \text{ Hz} \leq f \leq 6 \text{ Hz}$. The latter two studies are both based on the site classification by Lee *et al.* [2001]. As mentioned below the classification is not correct for numerous stations. Clearly, Sokolov *et al.* [2004] provided the model-based site effect, and the others gave the reference-site-based one.

[5] In Taiwan, a project of exploring the geological and seismic velocity structures beneath strong-motion stations has been launched by the Central Weather Bureau (CWB) and conducted by the National Center for Research on Earthquake Engineering (NCREE) since 2000. Borehole loggings are made for measuring the density (ρ), the specific gravity, the P-wave velocity (V_p), and the S-wave (shear) velocity (V_s), at different depths. At the holes, which were drilled in 2000, the depth (denoted by d_B hereafter) is less than 30 m, because the holes are located at the rock sites. At most sites the d_B is equal to or larger than 30 m. In central Taiwan, in which the 1999 $M_s 7.6$ Chi-Chi earthquake was located, there are 87 boreholes, which are located at two different geological provinces, as shown in Figure 1.

[6] In this study, from well-logging data of shear velocities and densities we evaluate the amplifications at the 87 borehole sites using the method proposed by Boore and Joyner [1997]. Also estimated are the averaged amplifications for the three classes of sites.

2. Method

[7] Joyner *et al.* [1981] first introduced the quarter-wavelength approximation method to evaluate the frequency-dependent site effect. At a particular frequency, the amplification is the square root of the ratio of seismic impedance (velocity times density) averaged over a depth range associated with a quarter wavelength to that at the depth of the source of seismic waves. Day [1996] made some theoretical justification on the method. The approximation is insensitive to the discontinuities in seismic velocities beneath a site, and the method does not include the nonlinear response due to the different input intensities of seismic waves and the resonance due to subsurface topography.

[8] In the quarter-wavelength approximation, the incident-plane waves through attenuation corrections are taken into account. Boore and Joyner [1997] defined the amplification to be the ratio of the Fourier amplitude spectrum of

¹Graduate Institute of Geophysics, National Central University, Jung-Li, Taiwan.

²Institute of Earth Sciences, Academia Sinica, Nangang, Taipei, Taiwan.

³National Center for Research on Earthquake Engineering, Taipei, Taiwan.

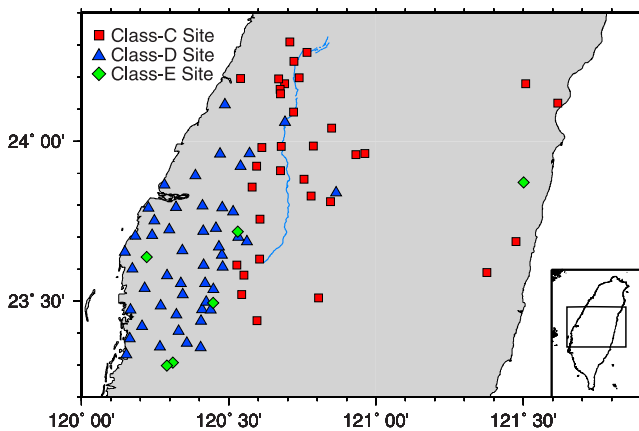


Figure 1. The station sites in use: squares, triangles, and diamonds for Class-C, D, and E sites, respectively. A blue solid line shows the Chelungpu fault.

un-attenuated incident-plane waves to that recorded at the surface of a uniform half-space by the same incident waves. The amplification therefore approaches unity for very long-period waves. They defined $S_H(z)$ to be the average S-wave travel time, $\beta(z) = z/S_H(z)$ the average velocity, $\rho(z)$ the average density, $f(z) = 1/[4S_H(z)]$ the frequency associated with the layer thickness of z , and $A(f) = [\rho_s \beta_s / \rho(z) \beta(z)]^{1/2}$, where the subscript “s” represents the source area, the amplification. The five quantities are calculated from the surface to depth z .

3. Borehole Data

[9] In Taiwan, a project has been launched by the CWB and conducted by NCREC to perform well-loggings near strong-motion station sites since 2000. There are 87 boreholes, which are shown in Figure 1, in central Taiwan. Obviously, 82 sites are on the western part of central Taiwan, and only five in eastern one. There is no station in the middle part, which is the Central Range. Figure 2a shows frequency distribution of depth of the 87 boreholes. The majority of the boreholes have a depth of 30 m. The depths of 78 boreholes are less than 40 m. The deepest borehole has a depth of about 150 m. The core samples of the 87 sites show that the major geological materials are the clay of high plasticity, silty soils, silty sand, sand-silt mixture et al. The formations of the core samples belong to three geological time periods, i.e., the Holocene, Pliocene, and Miocene.

[10] The shear velocities and densities were measured at each borehole. The shear velocity was measured every 0.5 m in each hole. The total number of samples of loggings for shear velocity is 6163 and the measured shear velocity is in the range 100–900 m/s. The US’s criteria to classify sites [cf. Lee *et al.*, 2001] are based on shear velocities, V_s : $V_s > 1500$ m/sec for Class-A sites, $V_s = 760$ –1500 m/s for Class-B ones, $V_s = 360$ –760 m/s for Class-C ones, $V_s = 180$ –360 m/s for Class-D ones, and $V_s < 180$ m/s for Class E ones. Based on the criteria, Lee *et al.* [2001] classified the 708 free-field strong-motion station sites from surficial geology. However, from the well-logging data, their classification is wrong for numerous sites. In central Taiwan, the classes of 65 station sites must be revised: Two Class-B stations are re-classified

into Class-C ones; 1 of 6 Class-C stations into Class-D one; 24 of 38 Class-D stations into Class-C ones; 2 of 38 Class-D stations into Class-E ones; 1 of 39 Class-E stations into Class-C one; and 35 of 39 Class-E stations into Class-D ones. Hence, there are 33 Class-C sites (denoted by squares), 48 Class-D ones (shown by triangles), and 6 Class-E ones (depicted by diamonds). In western Taiwan, the Class-C sites are located mainly in the Western Foothill with Pleistocene and Miocene formations, and the Class-D and E sites in the Western Plain with thick Holocene alluvium.

[11] The density was not measured regularly every 0.5 m and only done at one point in a certain geological layer. The total number of samples of loggings for density is 1468 and the measured density is in the range 1.5–2.5 gm/cc. Obviously, at some well-logging points, where the shear-velocity was measured, there is lack of density. At such a point, the density measured at a nearby one, which belongs to the same geological layer as the former, is assigned. A complete well-logging profile including the two parameters can, thus, be constructed at each site.

[12] An important site factor in predicting ground motions and in constructing the building codes [cf. Boore and Joyner, 1997] is the averaged shear velocity from the ground surface to 30-m depth, i.e., $V_{30} = 30/S_H(30)$. Theoretically, $S_H(d)$ is the integral of $z/\beta(z)$ from the surface to the depth d . In this study, $S_H(d)$ is the sum of the values of $z/\beta(z)$ at numerous depths, separated by a small interval, e.g. 0.5 m. Since $d_B < 30$ m for a few boreholes, the calculations of S_H are different for $d_B < 30$ m and for $d_B \geq 30$ m. When $d_B \geq 30$ m, the $S_H(30)$ is the sum of $0.5/\beta(z)$ within the 30-m depth. When $d_B < 30$ m, the value of $S_H(d_B)$, which is the sum of $0.5/\beta(z)$ within d_B , is extrapolated to $S_H(30)$ using a power-law function as explained below. Figure 2b displays the frequency distribution of V_{30} . There are two groups with different peaks: the first one with a peak around 450 m/s for Class-C sites and the other with a peak near 250 m/s for Class-D and E ones. The distribution is more dispersed for Class-C sites than Class-D and E ones.

4. Amplifications From Borehole Data

[13] In order to evaluate the amplifications as functions of depth, it is necessary first to construct the depth functions of $S_H(z)$. Results are depicted in Figure 3, with the least-squares fits displayed by dashed lines. Obviously, the depth functions of $S_H(z)$ can be divided into three groups, each associated with a class of sites, which are shown with different kinds of color: red for Class-C sites, blue for

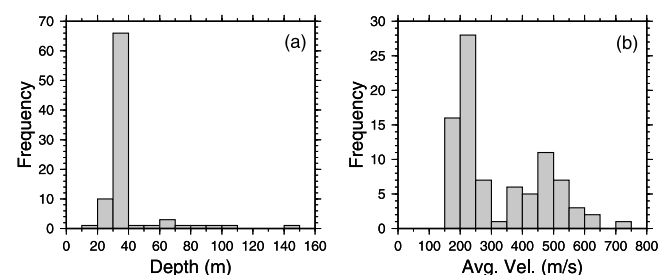


Figure 2. (a) Histogram for depths of boreholes and (b) histogram of shear velocity averaged over the upper 30 m from well-loggings.

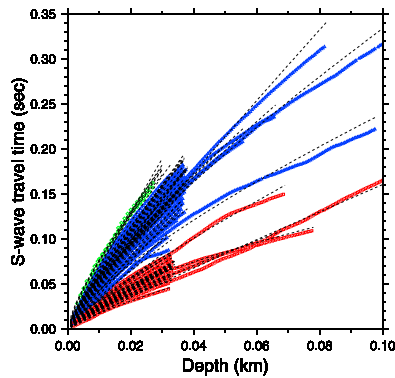


Figure 3. S_{II} versus depth: red, blue, and green for Class-C, D, and E sites, respectively. The least-squares fit of a power law is given by a dashed line.

Class-D ones, and green for Class-E ones. In order to calculate V_{30} , extrapolation must be made for estimating the value $S_{II}(z)$ at $z = 30$ m from the least-squares fit at the boreholes with a depth of being less than 30 m.

[14] Two deep boreholes with depths of 455.3 and 211.2 m, respectively, were drilled near the Chelungpu fault (see Figure 1) [Tanaka *et al.*, 2002]. The densities measured from the loggings increase gradually with depth, reaching a value of about 2.8 gm/cc, which is taken to be ρ_s . From Ma *et al.* [1996], the average crustal shear velocity, i.e., 3500 m/s, is taken to be β_s .

[15] First, from $\beta(z)$ and $\rho(z)$ we calculate $A[f(z)]$ and $f(z)$ at a single borehole. The results are displayed in Figure 4 with different light open symbols: squares, triangles, and diamonds, respectively, for Class-C, D, and E sites. Secondly, we compute average $A[f(z)]$ for a class of sites from the values of $A[f(z)]$ at all boreholes of the class at the same depth. Results are given in Table 1. Obviously the numbers of logging data for Class-E sites are small. At low frequencies, such numbers for Class-C and D sites are also small. The data points of average $A[f(z)]$ versus average $f(z)$ are displayed in Figure 4 with solid symbols: squares, triangles, and diamonds, respectively, for Class-C, D, and E sites. Included also in Figure 4 are the error bars for both $A[f(z)]$ and $f(z)$. Essentially, average $A[f(z)]$ increases with average $f(z)$ for the three classes of sites. The values of average $A[f(z)]$ approach 3.8, 5.5, and 6.1, respectively, for Class-C, D, and E sites when $f(z) > 10$ Hz.

[16] The frequency ranges are different for the three classes of sites. The $V_{30} = 30/S_{II}(30)$ (in m/s) controls the magnitude of lower-bound frequency, f_{low} , associated with the topmost 30-m layer. The V_{30} is: 383.9–709.0 m/s, 185.8–359.1, and 158.3–175.0 m/s for Class-C, D, and E sites, respectively. The related f_{low} is: 3.0–5.9 Hz, 1.5–3.0 Hz, and 1.3–1.5 Hz for Class-C, D, and E sites, respectively. In Figure 4, for Class-C sites, except for few boreholes with $d_B > 30$ m, there are no data points for $f(z) < 2$ Hz. The plots can be divided into three groups, associated with Class-C, D, and E sites, respectively, from top to bottom. The plots of Class-D and E are close to each other.

5. Discussion

[17] Figure 3 shows that the $S_{II}(z)$ increases with depth almost in a power-law form, i.e., $S_{II}(z) \sim z^n$, which is

depicted by a dashed line in Figure 3. The n varies site by site, with the largest one at a Class-E site, the second largest one at a Class-D site, and the smallest one at a Class-C site.

[18] Figure 4 shows that the amplification-frequency functions of the three classes of sites all increase with frequency. However, the functions become flat when $f > 10$ Hz. The amplification functions reflect the effects due to geological characteristics: those for $f < 1$ Hz from the velocity structure with $z > 30$ m and those for $f > 1$ Hz from the structure with $z < 30$ m. Thus, flatness implicates a uniform velocity structure in the shallow part. The amplifications at Class-D sites are about 1.7 times larger than those at Class-C ones. The amplifications at Class-E sites are about 1.2 times larger than those at Class-D ones. As mentioned above, almost all Class-C sites are located at the Western Foothill with Pleistocene and Miocene formations, and the Class-D and E sites in the Western Plain with Holocene alluvium. The shear velocities and densities are higher in Class-C sites than in Class-D and E ones, thus leading to smaller amplifications in the former sites than in the latter ones. Now, a solid correlation between site amplification and local geology cannot be delineated due to high complexity of local geology.

[19] According to a very-hard-rock model, Sokolov *et al.* [2004] evaluated the amplifications in the frequency range 0.1–10 Hz from seismograms over the whole Taiwan region. They calculated the Fourier spectrum from $A(f) = (2\pi f)^2 CS(f)D(r, f)I(f)$, where C = scaling factor, $S(f)$ = source spectrum, $D(r, f)$ = attenuation function, $I(f)$ = instrumental response, and r = hypocentral distance. $D(r, f)$ is $e^{-\pi f r / \beta Q(f)}$ times $e^{-\kappa \pi f}$, where $Q(f)$ is the quality factor and $e^{-\kappa \pi f}$ is the high-cut filter [Anderson and Hough, 1984]. They used $Q(f) = 80f^{0.8}$ obtained by Sokolov *et al.* [2002] for the shallow crustal structures and took $\kappa = 0.03$ sec. In this study, their amplifications are corrected by excluding high-cut filtration. The results of Class-C and D sites are displayed in Figure 4. There are errors in theirs due to miss-classification at some sites by Lee *et al.* [2001]. The lack of well-logging data below 1 Hz makes us unable to compare their results with ours for $f < 1$ Hz. At Class-C sites, our amplifications are lower for $2 \text{ Hz} \leq f \leq 6 \text{ Hz}$ and higher for $6 \text{ Hz} \leq f \leq 12.5 \text{ Hz}$ than theirs. At Class-D sites, ours are about 1.3 times higher than theirs at all frequencies in consideration.

[20] The possible reason to cause low $A[f(z)]$ at Class-D and E sites by Sokolov *et al.* [2004] is that their very-hard-

Table 1. The Values of $A(f)^a$

f , Hz	Classification		
	C	D	E
1.0		4.5(3)	
2.3	2.8(2)	4.9(45)	5.4(3)
3.1	3.1(4)	5.0(48)	5.6(4)
5.0	3.2(32)	5.2(48)	6.9(5)
11.0	3.5(32)	5.4(47)	6.2(5)
25.8			6.4(3)
28.8	3.7(31)		
29.7		5.6(46)	
39.6	3.7(32)		

^aThe numbers of boreholes at the same depth used in estimating $A(f)$ for the three classes of sites are given in the parentheses.

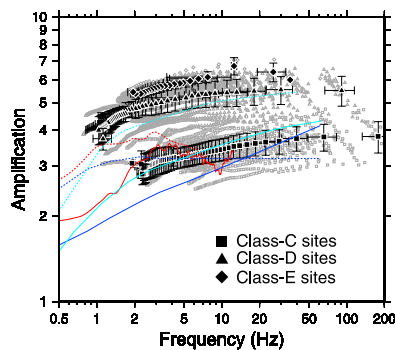


Figure 4. The plots of $A(f)$ versus f : squares, triangles, and diamonds for Class-C, D, and E sites, respectively. The average values, with error bars, are displayed by solid symbols. Included also are the results by others for Class-C (in solid lines) and Class-D (in dashed lines) sites: deep blue for *Boore and Joyner* [1997], light blue for *Klimis and Margaris* [1999], and red for *Sokolov et al.* [2004].

rock model, $Q = 80f^{0.8}$, might not be completely appropriate for the source area of seismic waves in the Western Plains with thick Holocene alluvium of several hundred meters [cf. *Ma et al.*, 1996]. In western Taiwan, which is slightly larger than the study area, *Wang* [1993] reported $Q = 95\text{--}110$ for $f = 2\text{--}6$ Hz. For this frequency range, $Q = 80f^{0.8}$, gives $Q = 139\text{--}335$, which are 2–3 times larger than the above-mentioned values. This seems able to explain low $A[f(z)]$ at Class-D and E sites, at least, for $f = 2\text{--}6$ Hz.

[21] Included also in Figure 4 are the $A(f)$ vs. f functions in Greece by *Klimis and Margaris* [1999] and those in North America by *Boore and Joyner* [1997]. For Class-C sites, the $A[f(z)]$ in Greece is slightly lower (larger) than ours when $f < 5$ Hz ($f > 5$ Hz); and the $A[f(z)]$ in North America are lower (larger) than ours when $f < 30$ Hz ($f > 30$ Hz). For Class-D sites, the $A[f(z)]$ in Greece is about 1.1 times smaller than ours, while the $A[f(z)]$ in North America is about 1.7 times smaller than ours. It is clear that the amplifications at Class-C and Class-D sites in central Taiwan are individually close to those in Greece. This might imply that the geological conditions in the two regions are similar. It is interesting that the $A[f(z)]$ at Class-C sites in central Taiwan are similar to that at Class-D sites in North America. The geological age in the study area is younger than that of the related regions in North America investigated by *Boore and Joyner* [1997]. The shear velocities of the same kind of rocks in the two regions are not necessarily equal. The result might implicate that it is either not appropriate to directly apply the criteria of site classification obtained from a region into another or the amplifications cannot be evaluated just based on surficial geology, that is, well-loggings are needed to evaluate the site amplifications.

[22] The natural frequency range for regular civil structures is 0.1–10 Hz. For a practical purpose, the amplifications at lower frequencies in the study area will be evaluated using a velocity model constructed from the well-logging data of a 2000-m borehole and

the 3D tomography inferred from P- and S-wave travel times.

6. Conclusions

[23] From the quarter-wavelength approximation method by *Boore and Joyner* [1997], we evaluate the frequency-dependent site amplifications at 87 free-field strong-motion stations in central Taiwan from well-logging data. Results show that the amplifications increase with frequency, and the amplification is larger at the sites in the Western Plain with thick Holocene alluvium than at those in the Western Foothill with Pleistocene and Miocene formations.

[24] **Acknowledgments.** The authors would like to express his thanks to Drs. Zollo, and Bonilla and an anonymous reviewer for constructive comments. This study was financially supported by Academia Sinica and the National Sciences Council under grant No. NSC94-2119-M-001-011.

References

- Anderson, J., and S. Hough (1984), A model for the shape of the Fourier amplitude spectrum of acceleration at high frequencies, *Bull. Seismol. Soc. Am.*, *74*, 1969–1993.
- Atkinson, G. M., and J. F. Cassidy (2000), Integrated use of seismograph and strong-motion data to determine soil amplification: Response of the Fraser River Delta to the Duvall and Georgia Strait earthquake, *Bull. Seismol. Soc. Am.*, *90*, 1028–1040.
- Boore, D. M., and W. B. Joyner (1997), Site amplifications for generic rock sites, *Bull. Seismol. Soc. Am.*, *87*, 327–341.
- Day, S. M. (1996), RMS response of a one-dimensional half space to SH, *Bull. Seismol. Soc. Am.*, *86*, 363–370.
- Joyner, W. B., R. E. Warrick, and T. E. Fumal (1981), The effect of Quaternary alluvium on strong ground motion in the Coyote Lake, California, earthquake of 1979, *Bull. Seismol. Soc. Am.*, *71*, 1333–1349.
- Klimis, N. S., and B. N. Margaris (1999), Site-dependent amplification functions and response spectra in Greece, *J. Earthquake Eng.*, *3*(2), 237–270.
- Lee, C.-T., C.-T. Cheng, C.-W. Liao, and Y.-B. Tsai (2001), Site classification of Taiwan free-field strong-motion stations, *Bull. Seismol. Soc. Am.*, *91*, 1283–1297.
- Lermo, J., and F. J. Chávez-García (1993), Site effect evaluation using spectral ratios with only one station, *Bull. Seismol. Soc. Am.*, *83*, 1574–1594.
- Ma, K.-F., J.-H. Wang, and D. Zhao (1996), Three-dimensional seismic velocity structure of the crust and uppermost mantle beneath Taiwan, *J. Phys. Earth*, *44*, 85–105.
- Pérez-Campos, X., S. K. Singh, and G. C. Beroza (2003), Reconciling teleseismic and regional estimates of seismic energy, *Bull. Seismol. Soc. Am.*, *93*, 2123–2130.
- Sokolov, V. Y., C.-H. Loh, and K.-L. Wen (2002), Comparison of the Taiwan Chi-Chi earthquake strong motion data and ground motion assessment based on spectral model from smaller earthquakes in Taiwan, *Bull. Seismol. Soc. Am.*, *92*, 1855–1877.
- Sokolov, V. Y., C.-H. Loh, and K.-L. Wen (2004), Evaluation of generalized site response functions for typical soil classes (B, C, and D) in Taiwan, *Earthquake Spectra*, *20*, 1279–1316.
- Tanaka, H., C.-Y. Wang, W.-M. Chen, A. Sakaguchi, K. Ujiie, H. Ito, and M. Ando (2002), Initial science report of shallow drilling penetrating into the Chelungpu Fault zone, Taiwan, *Terr. Atmos. Oceanic Sci.*, *13*, 227–251.
- Wang, J. H. (1993), Q values of Taiwan: A review, *J. Geol. Soc. China*, *36*, 15–24.
- Zhang, F. (2004), Site response and attenuation analysis using strong motion and short-period data, Ph.D. dissertation, 278 pp., Dep. Civ. Struct. Environ. Eng., State Univ. of N. Y., Buffalo.
- H.-H. Hsieh, National Center for Research on Earthquake Engineering, 200, Sec. 3, HsinHai Road, Taipei 106, Taiwan.
- M.-W. Huang, K.-F. Ma, and K.-L. Wen, Graduate Institute of Geophysics, National Central University, Jung-Li 320-54, Taiwan. (mwhuang@earth.sinica.edu.tw)
- J.-H. Wang, Institute of Earth Sciences, Academia Sinica, P.O. Box 1-55, Nangang, Taipei, 115, Taiwan.